Materials Letters 160 (2015) 423–427

Contents lists available at ScienceDirect

Materials Letters

journal homepage: www.elsevier.com/locate/matlet

MLBLUED1501295

Electrospinning superhydrophobic–superoleophilic fibrous PVDF membranes for high-efficiency water–oil separation

Zhengping Zhou, Xiang-Fa Wu *

Department of Mechanical Engineering, North Dakota State University, Fargo, ND 58108-6050, USA

ARTICLE INFO

Article history:
Received 23 March 2015
Received in revised form
26 June 2015
Accepted 2 August 2015
Available online 3 August 2015

Keywords:
Superhydrophobicity
Electrospinning
Poly (vinylidene fluoride) (PVDF)
Fibrous membranes
Emulsified oil/water solution
Water–oil separation

ABSTRACT

Ultrathin superhydrophobic–superoleophilic fibrous poly (vinylidene fluoride) (PVDF) membranes were prepared by means of electrospinning technique for the purpose of low-cost, high-efficiency water–oil separation. The ultrathin electrospun fibrous PVDF membranes exhibited a high water contact angle up to 153° and nearly zero oil (diesel) contact angle. The surface morphology and hydrophobicity of the membranes can be conveniently tuned by adjusting the PVDF concentration of the electrospinning solutions. The obtained ultrathin fibrous PVDF membranes showed excellent performance in separation of water-in-oil emulsions.

1. Introduction

Superhydrophobic surface is defined as a surface carrying the water contact angle greater than 150° and low contact angle hysteresis [1–4]. Research of superhydrophobic surfaces belongs to an interdisciplinary field of surface physics, surface chemistry and materials science and engineering, which has drawn extensive scientific and industrial interests due to the fact that a variety of applications can be traced to superhydrophobic surfaces such as self-cleaning, antifouling, corrosion resistance, anti-icing, oil/water filtration, etc. [5–9]. It has been well studied that the superhydrophobic property of lotus leafs is mainly controlled by two key surface parameters, i.e., the surface energy and surface roughness [2,10,11]. Accordingly, a superhydrophobic surface can be rationally designed and fabricated via modifying the rough surface of a low surface-energy material or decreasing the surface energy of a rough surface [11,12].

To date, a number of techniques have been successfully formulated for creating rough surface textures, including plasma polymerization/etching, inverse opal surface, layer-by-layer process, phase separation, sol–gel process, etc. [13–15]. Among others, electrospinning as a low-cost, continuous, scalable nanomanufacturing technique has been extensively employed for producing continuous nano-/microfibers of a large variety of natural and synthetic polymers, polymer derived carbon, metals, metal oxides and ceramics, etc. [16–28]. In addition, the surface morphology and mechanical properties of electrospun fibers can be tailored via adjusting the solution properties and the process parameters of electrospinning such as the solution conductivity, polymer molecular weight and concentration, applied electrical field, distance from the spinneret to the fiber collector, inner diameter of the spinneret, solution feeding rate, etc. [29–33].

In recent years, poly (vinylidene fluoride) (PVDF) has been under intensive investigation for producing superhydrophobic membranes due to its favorable properties such as the low surface energy (25 dynes cm^{-1}), sound chemical inertness, very good thermal stability, and high mechanical strength [12,34,35]. For instance, Jiang's group [35] has synthesized several types of superhydrophobic–superoleophilic PVDF membranes by means of phase-inversion process. These PVDF membranes showed a high water contact angle up to 158° and an oil contact angle less than 1°. Sigmund et al. [36] have fabricated a type of amorphous fluoropolymer (AF)-PVDF core–shell fibrous mat with the water contact angle higher than 150°. In addition, to achieve superhydrophobic surfaces, Ganesh et al. [3] reported to spin-coat fluorinated polyhedral oligomeric silsesquioxanes-poly (vinylidene fluoride-co-hexafluoro propylene) (fluoro POSS–PVDF–HFP) nanocomposite onto the glass surface by electrospinning. The fabricated surface showed a high water contact angle of 157.3° and a low sliding angle (< 5°). Recently, nonwoven fibrous membranes made of pure electrospun PVDF nanofibers have also been reported, which exhibited hydrophobic behavior with the water contact angle of 136° [37]. In order to further improve the

* Corresponding author. Fax: +1 701 231 28913.
E-mail address: Xiangfa.Wu@ndsu.edu (X.-F. Wu).

http://dx.doi.org/10.1016/j.matlet.2015.08.003
0167-577X/

hydrophobicity of these nanofibrous membranes, inorganic nanoparticles (e.g., SiO_2, TiO_2 and Al_2O_3) have been considered to incorporate into the PVDF nanofibers during the electrospinning process [38]. However, due to the weak bonding strength between the nanoparticles and PVDF nanofibers, these nanoparticles could be easily detached from the fibers.

In the present experimental study, we were going to fabricate nonwoven superhydrophobic–superoleophilic fibrous PVDF membranes in a single-step process via electrospinning PVDF solution with a mixture solvent of *N,N*-dimethylformamide (DMF)/acetone. Contact angle measurements of the fibrous PVDF members demonstrated that the surface morphology and diameter of the electrospun PVDF fibers played a dominant role in governing the superhydrophobicity of the resulting ultrathin fibrous membranes. The ultrathin fibrous PVDF membranes were further utilized for low-cost, high-efficiency separation of water-in-oil emulsions. Discussions of dependencies of the contact angle and water–oil separation of the ultrathin PVDF fibrous membranes upon the surface morphology and diameter of the PVDF fibers were made. Conclusion of the present experimental research was drawn in consequence.

2. Experimental

PVDF powders (Mw=534,000), *N,N*-dimethylformamide (DMF, 99%) and acetone were purchased from Sigma-Aldrich Chemical Co. (St. Louis, MO, USA). All the materials were used as received without further purification. The PVDF powders were first dissolved in DMF at a certain concentration and stirred at 55 °C for 8 h until a transparent homogenous solution was obtained. Then, the PVDF/DMF solution was cooled down to the room temperature, and a calculated amount of acetone was added. The weight ratio of the DMF and acetone in the resulting PVDF/DMF/acetone solution was 1:1. The blend PVDF/DMF/acetone solution was stirred for another 4 h to ensure a complete dispersion of PVDF in the solvent.

To electrospin fibrous PVDF membranes, the PVDF/DMF/acetone solution was placed into a 10-mL plastic syringe installed with a stainless steel-needle as the spinneret. A digitally controlled syringe pump was used to feed the polymer solution into the needle tip at a constant feeding rate of 4 ml h^{-1}. A rotary aluminum disk with the diameter of 33 cm was electrically connected to the negative high-voltage DC power supply and used as the fiber collector. During the electrospinning process, the PVDF solution underwent a high DC electrical field of 80 kV m^{-1}. Such a high DC electrical field was generated by applying a positive voltage of 18 kV and a negative voltage of 2 kV to a 25 cm gap between the spinneret and the fiber collector. After electrospinning, a nonwoven PVDF fibrous mat was formed onto the rotary aluminum disk, which was peeled off as an ultrathin fibrous PVDF membrane. The thickness of the PVDF members was controlled around 100–200 μm by the electrospinning time, which was fixed around 1 h in the present study. The obtained ultrathin fibrous PVDF membranes were then dried in vacuum at 60 °C for 12 h to remove the residual solvent before any further characterization.

The surface morphology and fiber diameters of the as-electrospun fibrous PVDF membranes were characterized by using a field-emission scanning electron microscope (SEM, JEOL JSM-7600F). Prior to SEM examination of the fibrous membranes, the membrane specimens were sputter-coated with carbon to avoid possible charge accumulation onto the PVDF fibers during the test. The surface roughness was measured by using a NT3300 non-contact optical profiler (Wyko Veeco, Co.). Contact angles were measured using a contact-angle measurement setup (First Ten Angstroms: FTÅ 125) based on the static sessile drop mode at room temperature. The contact angle of each sample was determined by averaging the values of five continuous measurements.

To examine the water–oil separation capability of the fibrous PVDF membranes, a surfactant-free water-in-oil emulsion was prepared by mixing water and diesel in 1:9 v:v and having been sonicated for 2 h to form a milky emulsion. The droplet sizes of the water-in-oil emulsion were in the range from 5 μm to 25 μm. The fibrous PVDF membranes with the fiber diameters of 2.02 ± 0.31 μm were utilized as the filtration membranes for evaluating the capability for water–oil separation. During the water–oil separation test, the prepared water-in-oil emulsion was poured onto the fibrous PVDF membrane without external driving force. To evaluate the filtration efficiency of the fibrous PVDF membranes for the water-in-oil emulsion, the absorbance of the feeding solution, pure oil and filtrated oil were measured in the range of 350–800 nm by using an ultraviolet–visible (UV–vis) spectrophotometer (Varian Cary 5000).

3. Results and discussion

In this experimental study, fibrous PVDF membranes of nearly uniform thickness were successfully produced via electrospinning PVDF/DMF/acetone solutions. The addition of organic solvent acetone was to decrease the viscosity and surface tension of the electrospinning solutions due to the low viscosity and low density of acetone [1]. During the electrospinning process, the average diameter and surface morphology of the PVDF fibers can be controlled by adjusting the PVDF concentration in the solution. The representative SEM micrographs and diameter distributions of the fibrous PVDF membranes were shown Fig. 1 (A)–(E). It can be clearly observed that the average diameter of the as-electrospun PVDF fibers gradually increases from 0.57 ± 0.12 μm to 4.82 ± 0.72 μm with increasing PVDF concentration from 10% to 17.5%. Thus, a higher PVDF concentration in the electrospinning solution can result in the larger fiber diameters due to the stronger intermolecular interactions in the electrospinning PVDF/DMF/acetone solution.

High-resolution SEM micrographs of the individual PVDF fibers are shown in the insets. The surface morphology and diameter of the PVDF fibers varied with the PVDF concentration in the electrospinning solution. In the case of small-diameter PVDF fibers, as shown in Fig. 1 (A) and (B), the PVDF fibers carried relatively smooth surface morphologies. However, once the fiber diameter increased, as shown in Fig. 1 (C)–(E), the fiber surfaces exhibited remarkable roughness with the surface morphology in terms of nano- and micro-scale structures, which were responsible for the superhydrophobicity of the fiber surfaces. Such nano/micro-scale surface structures are crucial to achieving the fiber superhydrophobicity. Fig. 1 (F) shows the wetting behavior of water and oil (diesel) on the as-prepared fibrous PVDF membranes of varying fiber diameters (i.e., the PVDF concentration in the electrospinning solutions). As shown in the insets, the ultrathin fibrous PVDF membranes showed the highest water contact angle of 153° and an oil (diesel) contact angle of 0°, which indicates both the promising superhydrophobic and superoleophilic surface properties. In addition, the electrospun fibrous PVDF membranes carried excellent flexibility and in-planar strength, which makes the synthesized PVDF membrane a promising candidate for the purpose of water–oil separation.

The shear viscosities of the PVDF/DMF/acetone solutions were characterized using a TA ARG2 Rheometer (TA Instruments, New Castle, DE) in the range of shear rate from 0.1 to 628.3 s^{-1} at room temperature. Fig. 2 shows the variation of the kinetic viscosity of the PVDF/DMF/acetone solution with respect to the shear rate at five PVDF concentrations. Given a shear rate, the shear viscosity of the solution increases with increasing PVDF concentration.

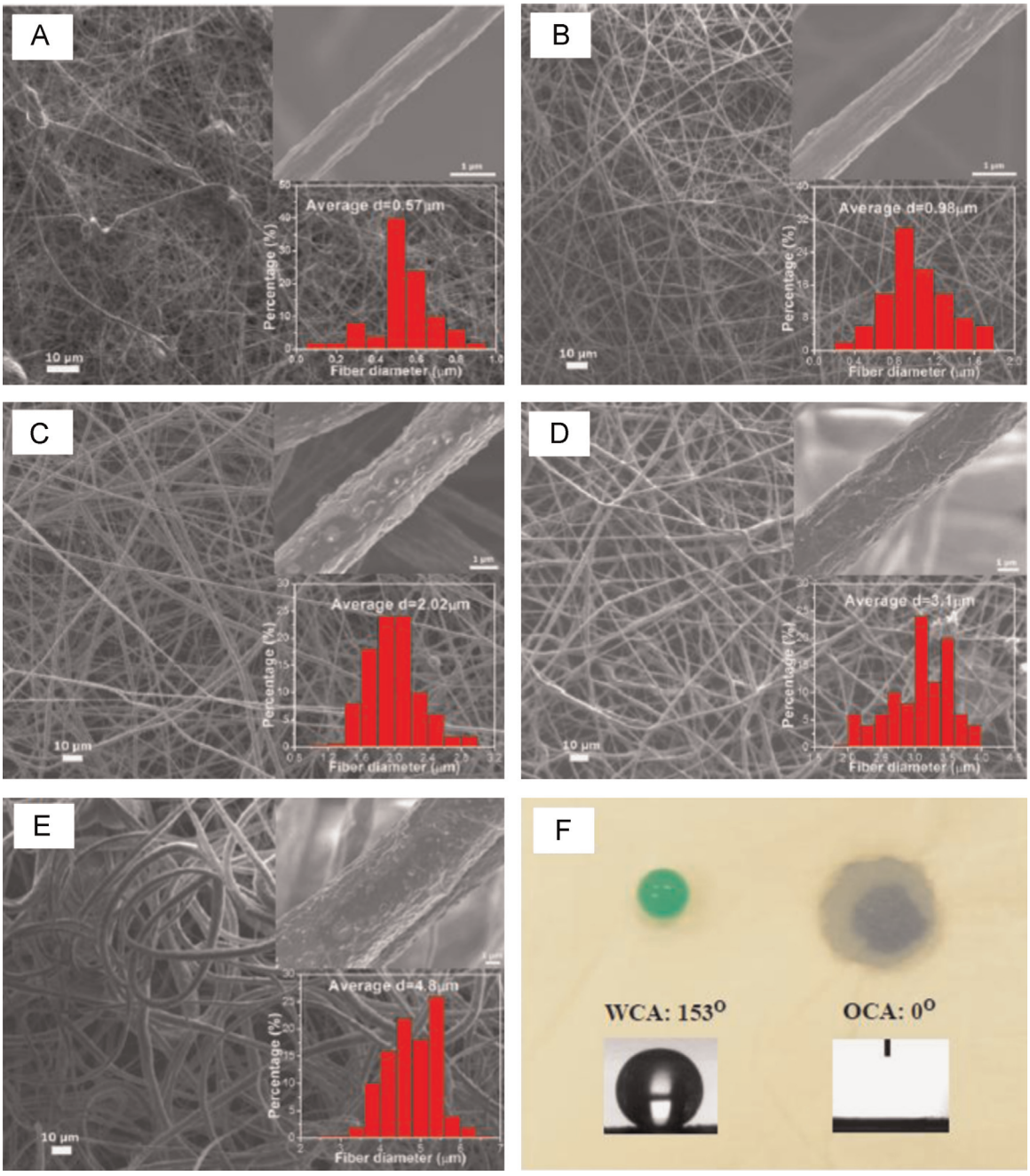

Fig. 1. (A)–(E) SEM micrographs of ultrathin fibrous PVDF membranes prepared via electrospinning PVDF/DMF/acetone solution of varying PVDF concentrations of 10%, 12.5 wt%, 15%, 16%, and 17.5%, respectively. The two insets in each SEM micrograph are the high-resolution SEM micrograph of an individual PVDF fiber and the fiber diameter distribution, respectively. (F) Optical image of an as-electrospun fibrous PVDF membrane with a water droplet showing a water contact angle of 153° (left) and a diesel oil droplet showing an oil contact angle of 0° (right).

Moreover, the shear viscosity decreases significantly with increasing shear rate at the high PVDF concentrations (e.g., 15%, 16% and 17.5%), while the shear viscosity is almost constant at the relatively low PVDF concentrations (e.g., 10% and 12.5%). Therefore, the experimental results of the shear viscosity indicate that the shear thinning behavior of the electrospinning solution became more and more obvious with increasing PVDF concentration. Given a polymer solution at the low polymer concentration, its solubility plays the dominant role in the viscosity. In contrast, at the high polymer concentration, the intermolecular interactions between the macromolecular chains dominate the mechanical behavior of a polymer solution. In addition, it is acknowledged that some experimental errors might be involved in viscosity measurements though it is not significant due to the evaporation of the solvent during the test that was performed within a small chamber.

The surface morphology and diameter of the PVDF fibers played a crucial role in the superhydrophobicity of the resulting ultrathin fibrous PVDF membranes. Variation of the static water contact angle and surface roughness with the diameter of the electrospun PVDF fibers is summarized in Fig. 3. Selected optical micrographs of the water droplets are shown in the insets. The obtained fibrous PVDF membranes at the fiber diameters of 0.57 ± 0.12 μm exhibited water contact angles of $145.1° \pm 0.9°$, which were much higher than those of flat monolithic PVDF membranes around ~90 ° [12]. As the diameter of the PVDF fibers

increases, the surface roughness of the fibrous PVDF membranes also increases and thereby enhances the water contact angle. As a result, the hydrophobicity of electrospun fibrous PVDF membranes increases monotonically up to an average water contact angle of about 151.7 ° ± 1.3 ° at the fiber diameters of 2.02 ± 0.31 μm. More importantly, all the fibrous PVDF membranes fabricated in this study maintained the high water contact angles (> 150 °), which carried the average fiber diameter and membrane surface roughness as high as 2.02 μm and 6.3 μm, respectively. The present results as shown in Fig. 3 can also approximately correspond to experimental results in the literature [37], where the water contact angles of electrospun PVDF nanofibers with the diameters in the range of 100–300 nm are lower than those of PVDF fibers with the diameters greater than 1 μm. The main reason is that at very small fiber diameter, the nanofiber mat become flat and roughness is limited; thus air bubble cannot be efficiently trapped. However, in the present case, the PVDF microfiber mats have hierarchal surface, i.e., the microfiber mat roughness and the microfiber surface roughness, which both contribute to the large water contact angle.

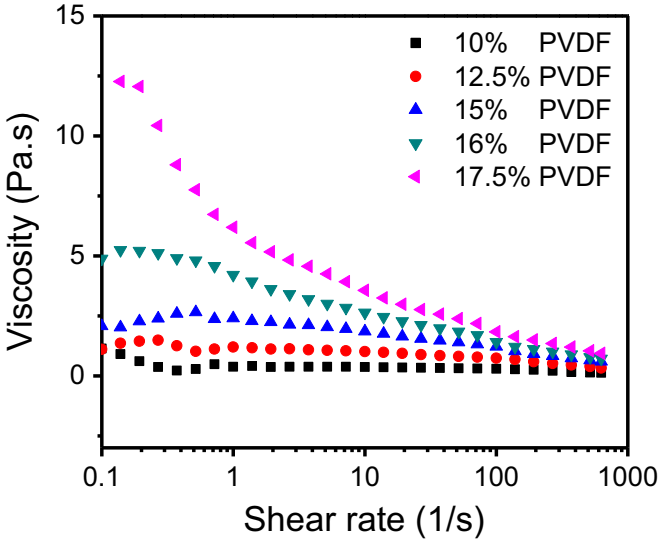

Fig. 2. Variation of the kinetic viscosity with respect to the varying shear rates for PVDF/DMF/acetone solutions with different PVDF concentrations.

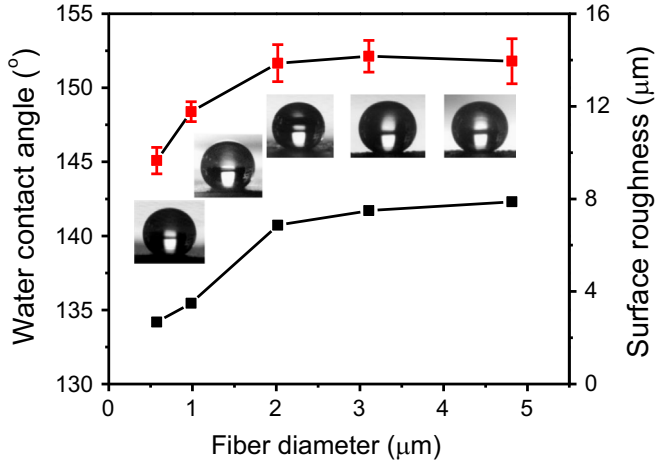

Fig. 3. Variations of the water contact angle and surface roughness of the fibrous PVDF membranes with the varying average diameters of electrospun PVDF fibers.

To test the water–oil separation capability of the electrospun fibrous PVDF membrane, a proof-of-concept liquid filtration and separation setup consisting of a Buchner funnel and a suction flask was built and used for the water–oil separation test [39,40]. During the filtration/separation test, a fibrous PVDF membrane with an effective permeation area of 8.04 cm^2 was used as the filter. The surfactant-free water-in-oil (diesel) emulsion with the water droplets in micrometer scales were poured onto the fibrous PVDF membrane. Without any external driving force, the oil was able to quickly permeate through the fibrous PVDF membrane. In the meantime, the water droplets were demulsified once touching the fibrous membrane and the residual water was finally retained at the above. To demonstrate the effective water–oil separation, an optical microscope (IX 71 Olympus with the objective magnification of 40) was employed to examine the emulsified droplets in water-in-oil solution before and after the filtration process. As shown in Fig. 4, after filtration, no visible droplets could be detected in the permeated oil, indicating a high water–oil separation efficiency of the fibrous PVDF membranes for water-in-oil emulsions. The UV–vis absorbance curves of the present water-in-oil

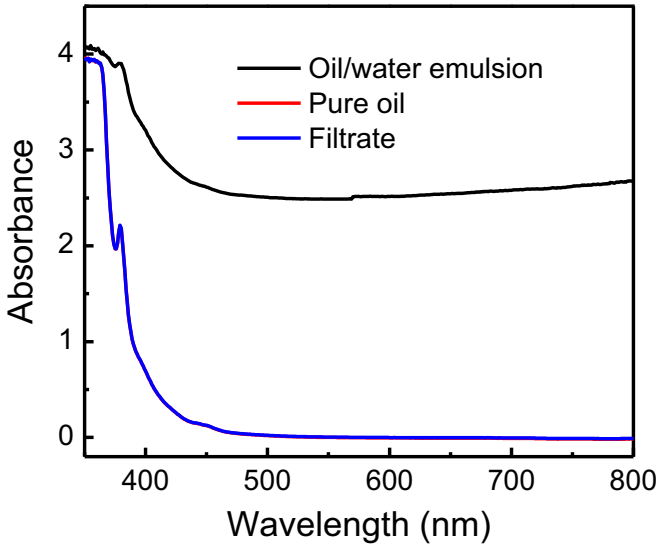

Fig. 5. UV–visible spectra of the water-in-oil emulsion, pure oil, and filtrated oil.

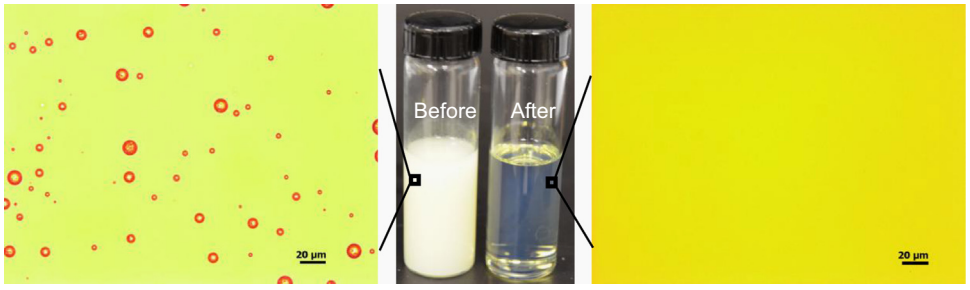

Fig. 4. Optical images of water-in-oil emulsion before and after filtration.

emulsion, pure oil (diesel), and filtrated oil were shown in Fig. 5. The filtrated oil curve can closely match the one of pure oil. These absorbance spectra further proved that the ultrathin electrospun fibrous PVDF membranes exhibited an excellent separation efficiency of 99.96% oil purity after filtration.

4. Concluding remarks

In this experimental study, ultrathin fibrous PVDF membranes with both superhydrophobic and superoleophilic properties were successfully fabricated by means of the low-cost electrospinning technique. The ultrathin electrospun fibrous PVDF membranes carried the highest water contact angle of 153° and an oil contact angle of 0°. The superhydrophobicity and superoleophility of the electrospun fibrous PVDF membranes are governed by the surface morphology and diameter of the PVDF fibers, which can be rationally controlled by adjusting the PVDF concentration in the electrospinning solution. Furthermore, the present investigation has also showed that electrospun fibrous PVDF membranes can be used as high-efficiency liquid separation membranes for separating emulsified water-in-oil solutions. In consequence, electrospinning technique as a low-cost, continuous, scalable fiber-manufacturing technique can be utilized for producing porous, flexible, high-strength fibrous PVDF membranes for use in water–oil separation.

Acknowledgment

Partial support of the research by the National Science Foundation (Grant CMMI-1234297) of the United States and the NDSU Development Endowment Fund (FAR0021589) is gratefully acknowledged. Z. Zhou thanks the North Dakota EPSCoR Doctoral Dissertation Fellowship Award (2013–2014). The membrane contact angle and UV absorbance were measured using the First Ten Angstroms (FTÅ 125) and the Varian Cary 5000, respectively, in Prof. D. Webster's group (Department of Coatings and Polymeric Materials at NDSU). The surface roughness was measured using an NT3300 non-contact optical profiler in the Center for Nanoscale Science and Engineering (CNSE) at NDSU. The shear viscosity of the solutions was measured using the ARG2 Rheometer in Prof. L. Jiang's group (ME Department at NDSU). The optical micrograph of the water-in-oil emulsion (Fig. 4) was taken using a high-resolution optical microscope in Prof. C. Sun's group (Department of Pharmaceutical Sciences at NDSU).

References

[1] C. Pan, Y. Hwang, L. Lin, Y. Chen, Design and Fabrication of Electrospun PVDF Piezo-Energy Harvesters, Wiley-IEEE Press, 2014.
[2] S. Michielsen, H. Lee, Langmuir 23 (2007) 6004–6010.
[3] A. Tuteja, W. Choi, J.M. Mabry, G.H. McKinley, R.E. Cohen, Proc. Natl. Acad. Sci. 105 (2008) 18200–18205.
[4] L. Feng, S. Li, Y. Li, H. Li, L. Zhang, J. Zhai, Y. Song, B. Liu, L. Jiang, D. Zhu, Adv. Mater. 14 (2002) 1857–1860.
[5] A. Nakajima, K. Hashimoto, T. Watanabe, K. Takai, G. Yamauchi, A. Fujishima, Langmuir 16 (2000) 7044–7047.
[6] R. Blossey, Nat. Mater. 2 (2003) 301–306.
[7] W. Choi, A. Tuteja, S. Chhatre, J.M. Mabry, R.E. Cohen, G.H. McKinley, Adv. Mater. 21 (2009) 2190.
[8] L. Mishchenko, B. Hatton, V. Bahadur, J.A. Taylor, T. Krupenkin, J. Aizenberg, ACS Nano 4 (2010) 7699–7707.
[9] P. Kim, T.S. Wong, J. Alvarenga, M.J. Kreder, W.E. Adorno-Martinez, J. Aizenberg, ACS Nano 6 (2012) 6569–6577.
[10] A. Tuteja, W. Choi, M.L. Ma, J.M. Mabry, S.A. Mazzella, G.C. Rutledge, G. H. McKinley, R.E. Cohen, Science 318 (2007) 1618–1622.
[11] M. Ma, Y. Mao, M. Gupta, K.K. Gleason, G.C. Rutledge, Macromolecules 38 (2005) 9742–9748.
[12] L. Zhai, F.C. Cebeci, R.E. Cohen, M.F. Rubner, Nano Lett. 4 (2004) 1349–1353.
[13] J.M. Lim, G. Yi, J.H. Moon, C.J. Heo, S. Yang, Langmuir 23 (2007) 7981–7989.
[14] Z. Gu, H. Uetsuka, K. Takahashi, R. Nakajima, H. Onishi, A. Fujishima, O. Sato, Angew. Chem. Int. Ed. 42 (2003) 894.
[15] H. Shang, Y. Wang, K. Takahashi, G. Cao, D. Li, Y. Xia, J. Mater. Sci. 40 (2005) 3587–3591.
[16] J. Doshi, D.H. Reneker, J. Electrostat. 35 (1995) 151–160.
[17] D.H. Reneker, I. Chun, Nanotechnology 7 (1996) 216–223.
[18] Z.M. Huang, Y.Z. Zhang, M. Kotaki, S. Ramakrishna, Compos. Sci. Technol. 63 (2003) 2223–2253.
[19] Y. Dzenis, Science 304 (2004) 1917–1919.
[20] D. Li, Y.N. Xia, Adv. Mater. 16 (2004) 1151–1170.
[21] D.H. Reneker, A.L. Yarin, E. Zussman, H. Xu, Adv. Appl. Mech. 41 (2007) 43–195.
[22] A. Greiner, J.H. Wendorff, Angew. Chem. Int. Ed. 46 (2007) 5670–5703.
[23] D.H. Reneker, A.L. Yarin, Polymer 49 (2008) 2387–2425.
[24] Z.P. Zhou, C.L. Lai, L.F. Zheng, Y. Qian, H.Q. Hou, D.H. Reneker, H. Fong, Polymer 50 (2009) 2999–3006.
[25] Z.P. Zhou, X.F. Wu, J. Power Sources 222 (2013) 410–416.
[26] Z.P. Zhou, X.F. Wu, J. Power Sources 262 (2014) 44–49.
[27] Z.P. Zhou, X.F. Wu, H.Q. Hou, RSC Adv. 4 (2014) 23622–23629.
[28] X.F. Wu, A. Rahman, Z.P. Zhou, D.D. Pelot, S. Sinha-Ray, B. Chen, S. Payne, A. L. Yarin, J. Appl. Polym. Sci. 129 (2013) 1383–1393.
[29] S.A. Theron, E. Zussman, A.L. Yarin, Polymer 45 (2004) 2017–2030.
[30] S.H. Tan, R. Inai, M. Kotaki, S. Ramakrishna, Polymer 46 (2005) 6128–6134.
[31] Z.P. Zhou, X.F. Wu, X.Q. Gao, L. Jiang, Y. Zhao, H. Fong, J. Phys. D 44 (2011) 435401.
[32] X.F. Wu, A.L. Yarin, J. Appl. Polym. Sci. 130 (2013) 2225–2237.
[33] Z.P. Zhou, X.F. Wu, Y.C. Ding, M. Yu, Y.H. Zhao, L. Jiang, C.L. Xuan, C.W. Sun, J. Appl. Polym. Sci. 131 (2014) 40896.
[34] F. Liu, N.A. Hashim, Y. Liu, M.R.M. Abed, K. Li, J. Membr. Sci. 375 (2011) 1–27.
[35] W. Zhang, Z. Shi, F. Zhang, X. Liu, J. Jin, L. Jiang, Adv. Mater. 25 (2013) 2071–2076.
[36] P. Muthiah, S.H. Hsu, W. Sigmund, Langmuir 26 (2010) 12483–12487.
[37] M. Wang, D. Fang, N. Wang, S. Jiang, J. Nie, Q. Yu, G. Ma, Polymer 55 (2014) 2188–2196.
[38] M. Sethupathy, V. Sethuraman, P. Manisankar, Soft Nanosci. Lett. 3 (2013) 37–43.
[39] M. Yu, Theoretical and experimental studies of droplets wetting on micro/nano-fibrous materials and their applications in oil–water separation (M.S. thesis), North Dakota State University, ND, USA, 2013.
[40] Z. Zhou, Synthesis and characterization of novel hierarchically functionalized carbon nanofibers for energy conversion and storage applications (Ph.D. thesis), North Dakota State University, ND, USA, 2014.